Mueller Matrix Elements That Characterize Scattering from Coated Random Rough Surfaces

Yuzhi Zhang and Ezekiel Bahar, *Fellow, IEEE*

***Abstract*— The Mueller matrix completely characterizes scattered electromagnetic waves. It relates the incident to the scattered Stokes vectors. The Mueller matrix, which contains intensity and relative phase data, is very useful for remote sensing. The Mueller matrix characterizing scattering from coated two-dimensional (2-D) random rough surfaces is obtained from full-wave solutions for the scattered fields considered in the companion paper. The general bistatic scattering case is considered in the analysis. However, for the numerical simluations presented here, the backscatter case is considered in particular, since backscatter is usually measured in remote sensing. The uniformly coated 2-D random rough surfaces are assumed here to be homogeneous and isotropic, with a Gaussian surface-height joint probability-density function. The diffuse incoherent and coherent contributions to the Mueller matrix elements are evaluated. The computer simulations of realistic models of relavent physical problems related to remote sensing of irregular stratified media can be used to determine the optimum modes of detection involving the selection of polarization, frequency, backscatter angle, and the specific Mueller matrix elements most sensitive to changes in medium parameters.**

***Index Terms*— Electromagnetic scattering, nonhomogeneous media.**

I. Introduction

THE modified Stokes vector is defined as follows [1]–[4]:

$$\mathbf{I}_M = \begin{bmatrix} I_1 \\ I_2 \\ U \\ V \end{bmatrix} = \begin{bmatrix} \langle E_1 E_1^* \rangle \\ \langle E_2 E_2^* \rangle \\ 2\mathrm{Re}\langle E_1 E_2^* \rangle \\ 2\mathrm{Im}\langle E_1 E_2^* \rangle \end{bmatrix}. \tag{1}$$

The modified Mueller matrix $\mathbf{M}$ that relates the incident (modified) Stokes vector $\mathbf{I}_M^i$ to the scattered (modified) Stokes vector $\mathbf{I}_M^f$ is defined as

$$\mathbf{I}_M^f = \mathbf{M}\mathbf{I}_M^i. \tag{2}$$

The elements of the normalized Mueller matrix $\mathbf{M}_n$, which are independent of the distance between the scatterer and the observation point, are defined by the following dimensionless quantities (consistent with the definition of the normalized radar cross sections [5]):

$$\langle S_0^{PQ} S_0^{RS^*} \rangle = \frac{4\pi (r^f)^2}{A_y} \frac{\langle E_s^P E_s^{R*} \rangle}{E_i^Q E_i^{S^*}} \tag{3}$$

where A_y is the radar footprint on the rough surface [3]. The expressions for the incoherent (normalized) modified Mueller matrix elements are

$$\mathbf{M}_n = [\mathbf{M}_{n1} \quad \mathbf{M}_{n2} \quad \mathbf{M}_{n3} \quad \mathbf{M}_{n4}] \tag{4a}$$

where $\mathbf{M}_{nj}$ $(j = 1, 2, 3, 4)$ are the following column matrices:

$$\mathbf{M}_{n1} = \begin{bmatrix} \langle S_0^{VV} S_0^{VV^*} \rangle_i \\ \langle S_0^{HV} S_0^{HV^*} \rangle_i \\ 2\mathrm{Re}\langle S_0^{VV} S_0^{HV^*} \rangle_i \\ 2\mathrm{Im}\langle S_0^{VV} S_0^{HV^*} \rangle_i \end{bmatrix} \frac{k_0^2}{\pi A_y} = \begin{bmatrix} m_{11} \\ m_{12} \\ m_{13} \\ m_{14} \end{bmatrix} \tag{4b}$$

$$\mathbf{M}_{n2} = \begin{bmatrix} \langle S_0^{VH} S_0^{VH^*} \rangle_i \\ \langle S_0^{HH} S_0^{HH^*} \rangle_i \\ 2\mathrm{Re}\langle S_0^{VH} S_0^{HH^*} \rangle_i \\ 2\mathrm{Im}\langle S_0^{VH} S_0^{HH^*} \rangle_i \end{bmatrix} \frac{k_0^2}{\pi A_y} = \begin{bmatrix} m_{21} \\ m_{22} \\ m_{23} \\ m_{24} \end{bmatrix} \tag{4c}$$

$$\mathbf{M}_{n3} = \begin{bmatrix} \mathrm{Re}\langle S_0^{VV} S_0^{VH^*} \rangle_i \\ \mathrm{Re}\langle S_0^{HH^*} S_0^{HV} \rangle_i \\ \mathrm{Re}\langle S_0^{VV} S_0^{HH^*} + S_0^{VH} S_0^{HV^*} \rangle_i \\ \mathrm{Im}\langle S_0^{VV} S_0^{HH^*} + S_0^{VH} S_0^{HV^*} \rangle_i \end{bmatrix} \frac{k_0^2}{\pi A_y} = \begin{bmatrix} m_{31} \\ m_{32} \\ m_{33} \\ m_{34} \end{bmatrix} \tag{4d}$$

$$\mathbf{M}_{n4} = \begin{bmatrix} -\mathrm{Im}\langle S_0^{VV} S_0^{VH^*} \rangle_i \\ -\mathrm{Im}\langle S_0^{HH^*} S_0^{HV} \rangle_i \\ -\mathrm{Im}\langle S_0^{VV} S_0^{HH^*} - S_0^{VH} S_0^{HV^*} \rangle_i \\ \mathrm{Re}\langle S_0^{VV} S_0^{HH^*} - S_0^{VH} S_0^{HV^*} \rangle_i \end{bmatrix} \frac{k_0^2}{\pi A_y} = \begin{bmatrix} m_{41} \\ m_{42} \\ m_{43} \\ m_{44} \end{bmatrix}. \tag{4e}$$

The symbol $\langle \cdot \rangle_i$ denotes the incoherent part of the (normalized) Mueller matrix element. It is defined as follows:

$$\langle S_0^{PQ} S_0^{RS^*} \rangle_i \equiv \langle S_0^{PQ} S_0^{RS^*} \rangle - \langle S_0^{PQ} \rangle \langle S_0^{RS^*} \rangle \tag{5}$$

and the statistical averaging is over the random rough surface heights and (large scale) slopes.

For the three media irregular layered structure (with a uniform coating over a random rough interface) considered in the companion paper [3], the scattering matrices are

$$\mathbf{S}_U = \int_{-L}^{L} \int_{-l}^{l} \frac{1}{c_0^f + c_0^i} \left[e^{i(\vec{k}_0^f - \vec{k}_o^i)\cdot \vec{r}_{s1}} - e^{i(\vec{k}_0^f - \vec{k}_o^i)\cdot \vec{r}_{s10}} \right] \times \mathbf{D}_U \mathbf{U}(\vec{n})\, dx_s\, dz_s \tag{6a}$$

$$\mathbf{S}_D = \int_{-L}^{L} \int_{-l}^{l} \frac{e^{i(\vec{k}_{1D}^f - \vec{k}_{1D}^i)\cdot \vec{r}_{s2}} - e^{i(\vec{k}_{1D}^f - \vec{k}_{1D}^i)\cdot \vec{r}_{s20}}}{c_1^i + c_1^f} \times \mathbf{D}_D \mathbf{U}(\vec{n})\, dx_s\, dz_s \tag{6b}$$

where

$$\mathbf{D}_U \equiv \mathbf{D}_{00U} + \mathbf{D}_{01U} e^{-i2v_1^i H_D} + \mathbf{D}_{10U} e^{-i2v_i^f H_D} + \mathbf{D}_{11U} e^{-i2(v_1^i + v_1^f) H_D} \tag{7a}$$

Manuscript received July 3, 1997; revised July 24, 1998.

The authors are with the Department of Electrical Engineering, Center for Electro-Optics, University of Nebraska-Lincoln, Lincoln, NE 68588 USA.

Publisher Item Identifier S 0018-926X(99)02861-6.

0018–926X/99$10.00 © 1999 IEEE

in which

$$\mathbf{D}_{00U} \equiv \mathbf{T}_0^f \mathbf{F}_{00U}^n \mathbf{T}_0^i \tag{7b}$$

$$\mathbf{D}_{01U} \equiv \mathbf{T}_0^f \mathbf{F}_{01U}^n \mathbf{T}_1^i \mathbf{T}_{10}^i \mathbf{R}_{21}^i \mathbf{R}^i \tag{7c}$$

$$\mathbf{D}_{10U} \equiv \frac{c_0^f}{c_1^f} \mathbf{R}^f \mathbf{R}_{21}^f \mathbf{T}_{01}^f \mathbf{T}_1^f \mathbf{F}_{10U}^n \mathbf{T}_0^i \tag{7d}$$

$$\mathbf{D}_{11U} \equiv -n_r \frac{c_0^f}{c_1^f} \mathbf{R}^f \mathbf{R}_{21}^f \mathbf{T}_{01}^f \mathbf{T}_1^f \mathbf{F}_{11U}^n \mathbf{T}_1^i \mathbf{T}_{10}^i \mathbf{R}_{21}^i \mathbf{R}^i \tag{7e}$$

and

$$\mathbf{D}_D = \mathbf{D}_{11D} \equiv \mathbf{R}^f \mathbf{T}_{10}^f \mathbf{T}_{1D}^f \mathbf{F}_{11D}^n \mathbf{T}_{1D}^i \mathbf{T}_{10}^i \mathbf{R}^i. \tag{7f}$$

In (7) $\mathbf{F}_{00U}^n$, $\mathbf{F}_{01U}^n$, $\mathbf{F}_{10U}^n$, $\mathbf{F}_{11U}^n$, $\mathbf{F}_{11D}^n$, the surface element scattering matrices (in the coordinate system associated with the large scale rough surface) $\mathbf{T}_0^i$, $\mathbf{T}_0^f$, $\mathbf{T}_1^i$, $\mathbf{T}_1^f$, $\mathbf{T}_{1D}^i$, $\mathbf{T}_{1D}^f$; the associated transformation matrices, and $\mathbf{R}^{f,i}$, $\mathbf{R}_{ab}^{f,i}$, $\mathbf{T}_{ab}^{f,i}$ are defined in the companion paper [3].

The elements of the 2×2 matrices $\mathbf{D}_K$ ($K = U, D$ and $a, b = 0, 1$) are associated with the like and cross polarized scattering coefficients D_K^{PQ} (7a), (7f) as follows:

$$\mathbf{D}_K \equiv \begin{bmatrix} D_K^{VV} & D_K^{VH} \\ D_K^{HV} & D_K^{HH} \end{bmatrix}, \quad (K = U, D). \tag{8}$$

The elements of the 2×2 matrices $\mathbf{D}_{abK}$ and $\mathbf{F}_{abK}^n (K = U, D; a, b = 0, 1)$ (7b)–(7e) are defined in a similar manner [3].

II. Evaluations of the Elements of the Modified Mueller Matrix

In this section, explicit expressions for the incoherent part of the Mueller matrix elements (4) are derived. A typical term in the expression for a Mueller matrix element is (5)

$$\begin{aligned} \langle S_0^{PQ} S_0^{RS^*} \rangle_i &= \langle (S_U^{PQ} + S_D^{RS}) (S_U^{PQ} + S_D^{RS})^* \rangle_i \\ &= \langle S_U^{PQ} S_U^{RS^*} \rangle_i + \langle S_U^{PQ} S_D^{RS^*} \rangle_i \\ &\quad + \langle S_D^{PQ} S_U^{RS^*} \rangle_i + \langle S_D^{PQ} S_D^{RS^*} \rangle_i. \end{aligned} \tag{9}$$

Thus, each incoherent term of a Mueller matrix element includes four (incoherent) terms involving scattering at the upper (U) and lower (D) interfaces $(UU, UD, DU,$ and $DD)$.

To facilitate the averaging over the surface height joint probability density function, the following assumptions are made.

1) The mean square (large scale) surface slopes are small ($\langle h_x^2 \rangle < 0.2$ and $\langle h_x^2 \rangle < 0.2$). The surface heights and slopes are assumed to be uncorrelated [5]

$$p(\vec{r}, \vec{n}', h_{s1}, h_{s1}') = p(\vec{r}, \vec{n}') p(h_{s1}, h_{s1}'). \tag{10}$$

2) The radii of curvature of the (large scale) rough surface is assumed to be large compared to the wavelength.
3) Since the scattering coefficients are slowly varying functions of the (large scale) surface slopes, the slopes at two neighboring points (within a correlation length) are aproximately the same [5].
4) The probability that a point on the surface is illuminated and visible depends on the slope of the surface at that point.
5) The random rough surfaces are assumed to be homogenous (surface statistics are independent of position) and isotropic (rough surface statistics are the same for all directions). Thus, the surface height autocorrelation function is only a function of distance.

The first term in (9) is expressed as follows (Appendix A):

$$\begin{aligned} \langle S_U^{PQ} S_U^{RS^*} \rangle_i = I_1 \int_{-2L}^{2L} \int_{-2l}^{2l} & (2l - |x_d|)(2L - |z_d|) \\ & \times [\chi_2(v_{y0}, -v_{y0}) - \chi(v_{y0})\chi(-v_{y0})] \\ & \times e^{i(v_{x0} x_d + v_{z0} z_d)} \, dx_d \, dz_d \end{aligned} \tag{11a}$$

where

$$\begin{aligned} I_1 &= \iint D_U^{PQ} D_U^{RS^*} P_2(\vec{n}^f, \vec{n}^i \mid \vec{n}) p(\vec{n}) \, d\vec{n} \\ &= {}_{00}^{00}IUU_{RS}^{PQ} + {}_{01}^{00}IUU_{RS}^{PQ} e^{i2v_1^{i*} H_D} + {}_{10}^{00}IUU_{RS}^{PQ} e^{i2v_1^{f*} H_D} \\ &\quad + {}_{11}^{00}IUU_{RS}^{PQ} e^{i2(v_1^{i*} + v_1^{f*}) H_D} + {}_{00}^{01}IUU_{RS}^{PQ} e^{-i2v_1^i H_D} \\ &\quad + {}_{01}^{01}IUU_{RS}^{PQ} e^{i2(v_1^{i*} - v_1^i) H_D} + {}_{10}^{01}IUU_{RS}^{PQ} e^{i2(v_1^{f*} - v_1^i) H_D} \\ &\quad + {}_{11}^{01}IUU_{RS}^{PQ} e^{i2(v_1^{f*} + v_1^{i*} - v_1^i) H_D} + {}_{00}^{10}IUU_{RS}^{PQ} e^{-i2v_1^f H_D} \\ &\quad + {}_{01}^{10}IUU_{RS}^{PQ} e^{i2(v_1^{i*} - v_1^f) H_D} + {}_{10}^{10}IUU_{RS}^{PQ} e^{i2(v_1^{f*} - v_1^f) H_D} \\ &\quad + {}_{11}^{10}IUU_{RS}^{PQ} e^{i2(v_1^{f*} + v_1^{i*} - v_1^f) H_D} \\ &\quad + {}_{00}^{11}IUU_{RS}^{PQ} e^{-i2(v_1^f + v_1^i) H_D} \\ &\quad + {}_{01}^{11}IUU_{RS}^{PQ} e^{i2(v_1^{i*} - v_1^f - v_1^i) H_D} \\ &\quad + {}_{10}^{11}IUU_{RS}^{PQ} e^{i2(v_1^{f*} - v_1^f - v_1^i) H_D} \\ &\quad + {}_{11}^{11}IUU_{RS}^{PQ} e^{i2(v_1^{f*} + v_1^{i*} - v_1^f - v_1^i) H_D}. \end{aligned} \tag{11b}$$

In (11)

$$\vec{k}_{dj} = \vec{k}_j^f - \vec{k}_j^i = v_{xj} \vec{a}_x + v_{yj} \vec{a}_y + v_{zj} \vec{a}_z \quad j = 0, 1 \tag{12a}$$

$\chi(a)$ and $\chi_2(a, b, R)$ are the characteristic and joint characteristic functions and

$$\begin{aligned} {}_{cd}^{ab}IUU_{RS}^{PQ} = \iint & D_{abU}^{PQ} D_{cdU}^{RS^*} p(\vec{n}) \\ & \times \sqrt{P_2(\vec{n}_a^f, \vec{n}_b^i \mid \vec{n}) P_2(\vec{n}_c^f, \vec{n}_d^i \mid \vec{n})} \, d\vec{n}. \end{aligned} \tag{12b}$$

In (12b), the shadow function $P_2(\vec{n}_a^f, \vec{n}_b^i \mid \vec{n})$, $(a, b = 0, 1)$ is the probability that a point on the rough surface is illuminated and visible (at the far field observation point) given the value of the slope at that point [7], [8]. For reflection from medium a back to medium a the shadow function is

$$P_2(\vec{n}_a^f, \vec{n}_a^i \mid \vec{n}) = \frac{U(-\vec{n}_a^i \cdot \vec{n}) U(\vec{n}_a^f \cdot \vec{n})}{\sqrt{1 + \frac{\Gamma_a^i}{u_a^i}} \sqrt{1 + \frac{\Gamma_a^f}{u_a^f}}} \qquad (a = 0, 1). \tag{13a}$$

For backscatter ($\vec{n}_a^f = -\vec{n}_a^i$) the above expressions are identically the same as those derived by Sancer and Smith [7], [8]. For transmission from medium a to medium b, the shadow function is

$$P_2(\vec{n}_b^f, \vec{n}_a^i \mid \vec{n}) = \frac{U(-\vec{n}_a^i \cdot \vec{n}) U(\vec{n}_b^f \cdot \vec{n})}{\sqrt{1 + \frac{\Gamma_a^i}{u_a^i}} \sqrt{1 + \frac{\Gamma_b^f}{u_b^f}}} \qquad (a, b = 0, 1). \tag{13b}$$

In (13), u_a^j and Γ_a^j are defined as follows:

$$u_a^j = \cos(\theta_a^j); \quad \Gamma_a^j = \int_{u_a^f}^{\infty} (h_x - u_a^j) p(h_x)\, dh_x \quad (j = i, f). \tag{14}$$

Similarly, the second term in (9) is

$$\langle S_U^{PQ} S_D^{RS^*} \rangle_i = I_2 \int_{-2L}^{2L} \int_{-2l}^{2l} (2l - |x_d|)(2l - |z_d|) \times [\chi_2(v_{y0}, -v_{y1}^*) - \chi(v_{y0})\chi(-v_{y1}^*)] \times e^{iv_{y1}^* H_D} e^{i(v_{x0}x_d + v_{z0}z_d)}\, dx_d\, dz_d. \tag{15a}$$

In (15a),

$$I_2 = {}_{11}^{00}IUD_{RS}^{PQ} + {}_{11}^{01}IUD_{RS}^{PQ} e^{-i2v_1^i H_D} + {}_{11}^{10}IUD_{RS}^{PQ} e^{-i2v_1^f H_D} + {}_{11}^{11}IUD_{RS}^{PQ} e^{-i2(v_1^i + v_1^f) H_D} \tag{15b}$$

where

$${}_{11}^{ab}IUD_{RS}^{PQ} = \iint D_{abU}^{PQ} D_{11D}^{RS^*} p(\vec{n}) \times \sqrt{P_2(\vec{n}_a^f, \vec{n}_b^i \,|\, \vec{n}) P_2(\vec{n}_{1D}^f, \vec{n}_{1D}^i \,|\, \vec{n})}\, d\vec{n}. \tag{15c}$$

The third term in (9) is

$$\langle S_D^{PQ} S_U^{RS^*} \rangle_i = I_3 \int_{-2L}^{2L} \int_{-2l}^{2l} (2l - |x_d|)(2l - |z_d|) \times [\chi_2(v_{y1}, -v_{y0}) - \chi(v_{y1})\chi(v_{y0})] \times e^{iv_{y1}^* H_D} e^{i(v_{x0}x_d + v_{z0}z_d)}\, dx_d\, dz_d. \tag{16a}$$

In (16a),

$$I_3 = {}_{00}^{11}IDU_{RS}^{PQ} + {}_{01}^{11}IDU_{RS}^{PQ} e^{i2v_1^{i*} H_D} + {}_{10}^{11}IDU_{RS}^{PQ} e^{i2v_1^{f*} H_D} + {}_{11}^{11}IDU_{RS}^{PQ} e^{i2(v_1^{i*} + v_1^{f*}) H_D} \tag{16b}$$

where

$${}_{cd}^{11}IDU_{RS}^{PQ} = \iint D_{11D}^{PQ} D_{cdU}^{RS^*} p(\vec{n}) \times \sqrt{P_2(\vec{n}_{1D}^f, \vec{n}_{1D}^i \,|\, \vec{n}) P_2(\vec{n}_c^f, \vec{n}_d^i \,|\, \vec{n})}\, d\vec{n}. \tag{16c}$$

The fourth term in (9) is

$$\langle S_D^{PQ} S_D^{RS^*} \rangle_i = I_4 \int_{-2L}^{2L} \int_{-2l}^{2l} (2l - |x_d|)(2l - |z_d|) \times [\chi_2(v_{y1}, -v_{y1}^*) - \chi(v_{y1})\chi(-v_{y1}^*)] \times e^{-i(v_{y1} - v_{y1}^*)} e^{i(v_{x0}x_d + v_{z0}z_d)}\, dx_d\, dz_d. \tag{17a}$$

In (17a)

$$I_4 = {}_{11}^{11}IDD_{RS}^{PQ} = \iint D_{11D}^{PQ} D_{11D}^{RS^*} p(\vec{n}) \times \sqrt{P_2(\vec{n}_{1D}^f, \vec{n}_{1D}^i \,|\, \vec{n}) P_2(\vec{n}_{1D}^f, \vec{n}_{1D}^i \,|\, \vec{n})}\, d\vec{n}. \tag{17b}$$

In (15)–(17), $\vec{n}_{1D}^i$, $\vec{n}_{1D}^f$, $\vec{n}_a^i$, and $\vec{n}_a^f (a = 0, 1)$ are the following unit vectors:

$$\vec{n}_{1D}^t = \frac{\mathrm{Re}[\vec{k}_{1D}^t]}{|\mathrm{Re}[\vec{k}_1^t]|} \quad (t = i, f) \tag{18a}$$

and

$$\vec{n}_0^t = \frac{\vec{k}_0^t}{k_0},\ \vec{n}_1^t \frac{\mathrm{Re}[\vec{k}_{1D}^t]}{|\mathrm{Re}[\vec{k}_1^t]|} \quad (t = i, f) \tag{18b}$$

where

$$\vec{k}_{1D}^t = k_1 [\sin\theta_1^t \cos\phi^t \vec{a}_x \pm \cos\theta_1^t \vec{a}_y + \sin\theta_1^t \sin\phi^t \vec{a}_z] \quad t = f \text{ upper sign; } t = i \text{ lower sign} \tag{18c}$$

and

$$\vec{k}_a^t = k_a [\sin\theta_a^t \cos\phi^t \vec{a}_x \pm \cos\theta_a^t \vec{a}_y + \sin\theta_a^t \sin\phi^t \vec{a}_z] \quad t = f, \quad a = 0 \quad \text{and} \quad t = i, \quad a = 1 \text{ upper sign}; \quad t = i \quad a = 1 \quad \text{and} \quad t = f, \quad a = 1 \text{ lower sign.} \tag{18d}$$

When medium 1 is dissipative, the vectors $\vec{k}_{1D}^i$, $\vec{k}_{1D}^f$, $\vec{k}_1^i$, and $\vec{k}_1^f$ are complex. In this case, the unit vectors (18) are taken to be in the direction of the average Poynting vector

$$\vec{P} = \frac{\mathrm{Re}[\vec{E} \times \vec{H}^*]}{2} = \mathrm{Re}\left[\frac{\vec{k}^*(\vec{E} \cdot \vec{E}^*)}{2\mu_0\omega}\right].$$

For homogenous, isotropic random rough surfaces

$$M_{13} = M_{14} = M_{23} = M_{24} = M_{31} = M_{32} = M_{41} = M_{44} = 0. \tag{19}$$

III. Illustrative Examples

In this section, the incoherent Mueller matrix elements are calculated for different random rough surfaces. For all the simulations, the two-dimensional (2-D) heights are homogeneous and isotropic. The surface height and slope probability density functions (pdf) are assumed to be Gaussian with Gaussian surface height autocorrelation functions, thus

$$p(h_s, h_s') = \frac{1}{2\pi\langle h_s^2 \rangle \sqrt{1 - R^2}} e^{-\left(\frac{h_s^2 - 2Rh_s h_s' + h_s'^2}{2\langle h_s^2 \rangle (1 - R^2)}\right)}. \tag{20}$$

In (20), $\langle h_s^2 \rangle$ is the surface mean square height and R is the normalized autocorrelation function

$$R = e^{-(r_d^2/l_c^2)} \tag{20c}$$

where $r_d = \sqrt{x_d^2 + z_d^2}$ is the distance between two points on the reference surface and l_c is the rough surface height autocorrelation length. The probability density function of surface slopes are

$$p(\vec{n}') = p(h_x, h_z) = \frac{1}{2\pi\sigma_s^2} e^{-\frac{h_x^2 + h_z^2}{2\sigma_s^2}} \tag{21}$$

where σ_s is the root mean square slope in the x and z directions and h_x and h_z are the derivatives of $h(x, z)$.

TABLE I
INPUT PARAMETERS FOR FIG. 1 (σ_s = CONSTANT)

σ_h (μ m)	l_c (μ m)	σ_s	H_D(μ m)	ε_{r1}	ε_{r2}
0.2	1.6293	0.1736	5	3	5
0.4	3.2586	0.1736	5	3	5
0.5	4.0732	0.1736	5	3	5
1	8.1464	0.1736	5	3	5

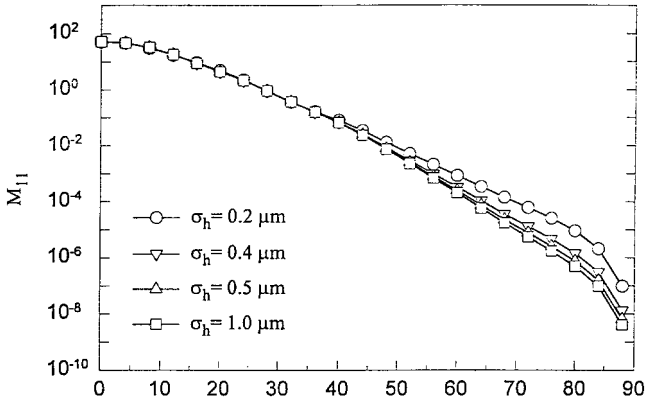

Fig. 1. Mueller matrix element M_{11} for rough surface with σ_s = constant.

The surface characteristic and joint characteristic functions for Gaussian pdf's are

$$\chi(a) = \exp\left(-\frac{\langle h_s^2\rangle a^2}{2}\right) \tag{22a}$$

and

$$\chi(a,b,R) = \exp\left(-\frac{\langle h_s^2\rangle (a^2+2abR+b^2)}{2}\right). \tag{22b}$$

For remote sensing, the computations of the modified Mueller matrix elements M_{ab} $(a,b = 1,2,3\,4)$ are usually carried out for backscatter. Thus, the incident and scatter elevation angles are equal. $\theta_0^i = \theta^f = \theta$ and the difference between the scatter and incident azimuth angles is $\phi^f - \phi^i = \pi$. For homogeneous and isotropic rough surfaces, there are only eight nonzero backscatter Mueller matrix elements. They are $M_{11}, M_{12} = M_{21}, M_{22}, M_{33}, M_{34}, M_{43}$, and M_{44}. When depolarization can be ignored, $M_{33} \approx M_{44}$ and $M_{34} \approx -M_{43}$.

The input parameters are the incident wavelength λ = 1.06 μm, the surface rms slope σ_s, the surface rms height $\langle h^2\rangle^{\frac{1}{2}} = \sigma_h, (l_c = \frac{\sqrt{2}\sigma_h}{\sigma_s})$, the thickness of the coating material, H_D, and the relative permittivities of media 1 and 2, ε_{r1} and ε_{r2}. Medium 0 is assumed to be free-space ($\varepsilon_{r0} = \mu_{r0} = 1$). Media 1 and 2 are nonmagnetic ($\mu_{r1} = \mu_{r2} = 1$).

For the input parameters given in Table I (σ_s = const) the Mueller matrix element M_{11} is plotted in Fig. 1. The elements M_{11}, $M_{12} = M_{21}$, and M_{22} are related to the normalized like and cross-polarized cross sections. They decrease monotonically with increasing backscatter angle θ. The cross polarized terms are $M_{12} = M_{21}$ (not shown) are about two orders smaller than the like polarized cross sections M_{11} (vertical) and M_{22} (horizontal, also not shown) is similar to M_{11}). The Mueller matrix elements $M_{33}, M_{44}, M_{34}, M_{43}$ (not shown)

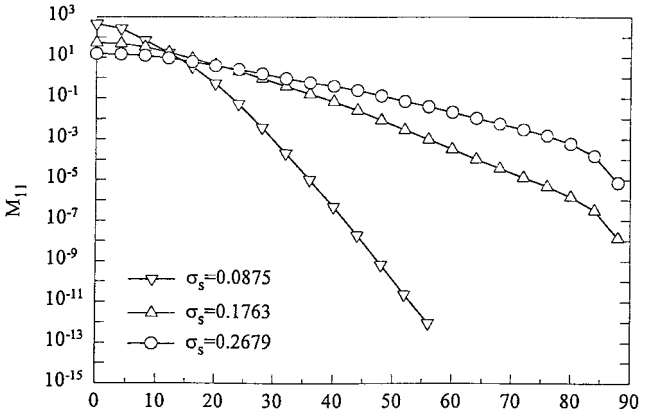

Fig. 2. Mueller matrix element M_{11} for rough surface with σ_h = constant.

TABLE II
INPUT PARAMETERS FOR FIG. 2 (σ_h = CONSTANT)

σ_h (μ m)	l_c (μ m)	σ_s	H_D(μ m)	ε_{r1}	ε_{r2}
0.4	1.6293	0.0875	5	3	5
0.4	3.2586	0.1736	5	3	5
0.4	4.0732	0.2679	5	3	5

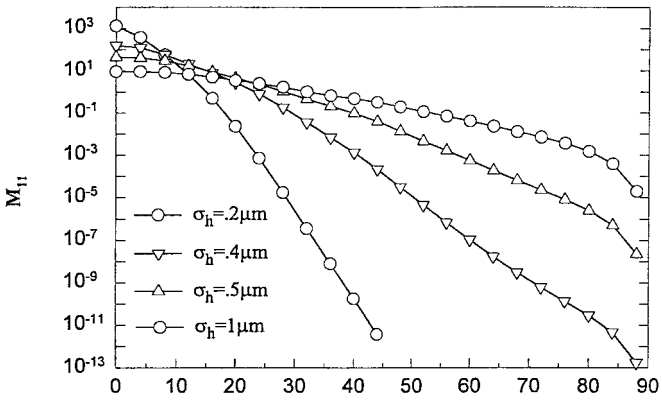

Fig. 3. Mueller matrix element M_{11} for rough surface with l_c = constant.

contain relative phase data $\psi^{VV} - \psi^{HH}$ (which is ≈180° at normal incidence).

The input parameters corresponding to the plots in Fig. 2 are given in Table II (σ_h = const). The Mueller matrix element M_{11} is much more sensitive to the variations in rms slope than to variations in rms height (Fig. 1). For the cases considered the larger the rms slopes, the smaller the values of M_{11}, $M_{12} = M_{21}$, and M_{22} at normal incidence. The plots for different rms slopes cross over at backscatter angles $\theta \approx 15°$ (for $\theta > 15°$, these Mueller matrix elements increase with increasing slope). At normal incidence the magnitudes of M_{33} ($\approx M_{44}$), M_{34} ($\approx -M_{43}$) (not shown) increase with decreasing slope and they vanish at near grazing angles.

For the plots of M_{11} in Fig. 3, the input parameters are listed in Table III (the autocorrelation length is constant). The results for this set of input data are similar to the previous results (rms heights constant) because the root mean square (rms) slopes ($\sigma_s = \sqrt{2}\frac{\sigma_h}{l_c}$) also vary for these cases.

The input parameters corresponding to the plots in Fig. 4(a) and (b) are listed in Table IV. The effects of varying the

TABLE III
INPUT PARAMETERS FOR FIG. 3 (l_c = CONSTANT)

σ_h (μ m)	l_c (μ m)	σ_s	$H_D(\mu$ m)	ε_{r1}	ε_{r2}
0.2	4.572	0.0618	5	3	5
0.4	4.572	0.1237	5	3	5
0.5	4.572	0.1547	5	3	5
1	4.572	0.3093	5	3	5

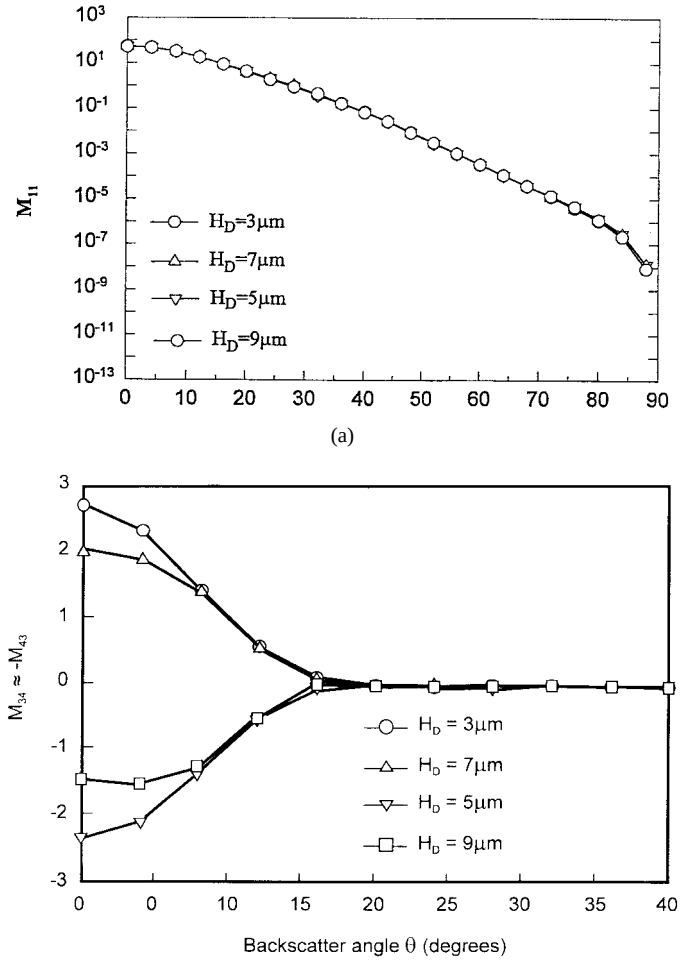

Fig. 4. (a) Mueller matrix element M_{11} for rough surfaces with $H_D = 3, 5, 7, 9$ μm. (b) Mueller matrix element M_{34} ($\approx -M_{43}$) for rough surfaces with $H_D = 3, 5, 7, 9$ μm.

TABLE IV
INPUT PARAMETERS FOR FIG. 4(a) AND (b) (H_D VARIES)

σ_h (μ m)	l_c (μ m)	σ_s	$H_D(\mu$ m)	ε_{r1}	ε_{r2}
0.4	3.2586	0.1736	3	3	5
0.4	3.2586	0.1736	5	3	5
0.4	3.2586	0.1736	7	3	5
0.4	3.2586	0.1736	9	3	5

thickness of the coating material (medium 1) are illustrated in Fig. 4(a) for M_{11}.

The Mueller matrix element M_{34} ($\approx -M_{43}$) Fig. 4(b) is most sensitive to changes in the thickness of the coating material as expected since the relative phase depends critically upon the thickness H_D. The sensitivity of M_{34} ($\approx -M_{43}$) to

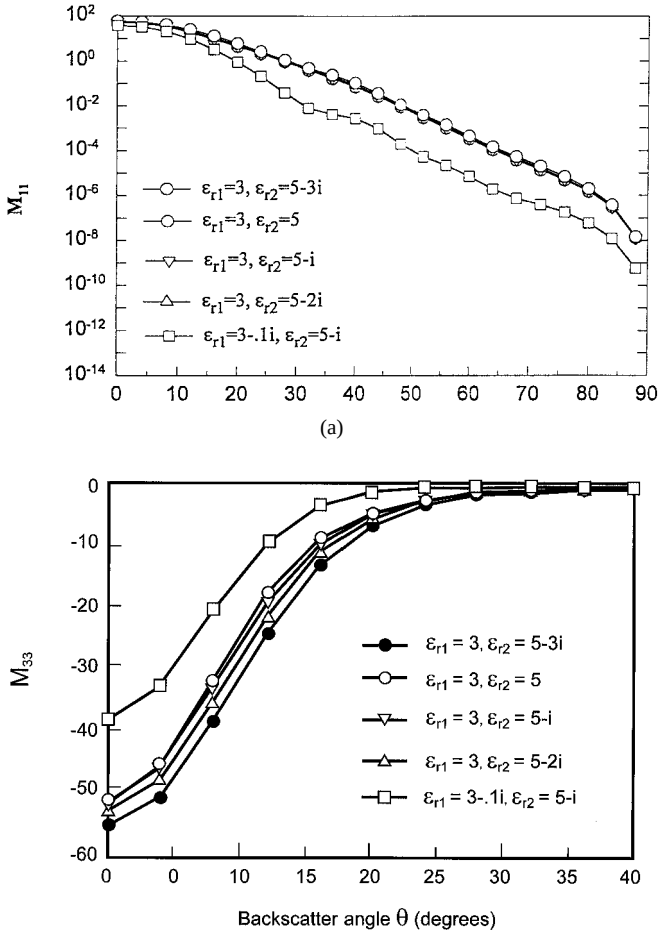

Fig. 5. (a) Mueller matrix element M_{11} for different permittivities. (b) Mueller matrix element M_{33} ($\approx -M_{44}$) for different permittivities.

TABLE V
INPUT PARAMETERS FOR FIG. 5(a) AND (b)
(PERMITTIVITIES OF MEDIA 1 AND 2 VARY)

σ_h (μ m)	l_c (μ m)	σ_s	$H_D(\mu$ m)	ε_{r1}	ε_{r2}
0.4	3.2586	0.1736	5	3	5
0.4	3.2586	0.1736	5	3	$5-i$
0.4	3.2586	0.1736	5	3	$5-2i$
0.4	3.2586	0.1736	5	3	$5-3i$
0.4	3.2586	0.1736	5	$3-0.1i$	$5-i$

coating thickness could be used to remotely sense the coating thickness. The other Mueller matrix elements are practically insensitive to the thickness H_D.

The effects of introducing dissipation to media 1 and 2 are examined in Fig. 5(a) and (b). The corresponding parameters are given in Table V. The Mueller matrix elements M_{11} [Fig. 5(a)] ($M_{12} = M_{21}$, and M_{22} not shown) are practically insensitive to variations in the dissipation in medium 2. However, the magnitudes of all the Mueller matrix elements decrease with increasing dissipation in medium 1. This is because waves are attenuated in medium 1 and the contributions from the multiple bounce terms in medium 1 decreases. The Mueller matrix elements related to horizontal and cross polarized cross sections M_{22} and M_{21} oscillate when medium

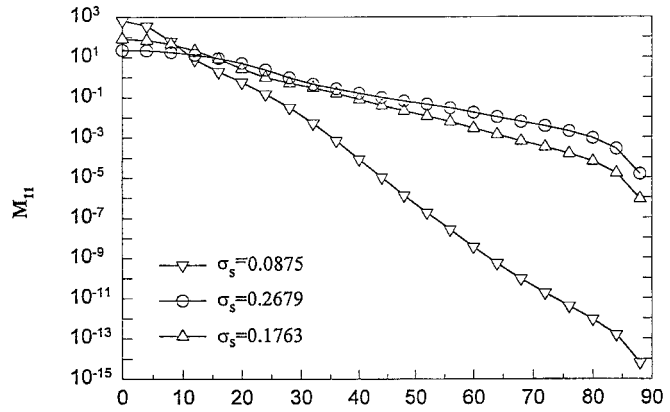

Fig. 6. Mueller matrix element M_{11} for rough surfaces with $\epsilon_{r1} > \epsilon_{r2}$ and (σ_h = constant).

TABLE VI
INPUT PARAMETERS FOR FIG. 6 ($\epsilon_{r1} > \epsilon_{r2}$ AND σ_h = CONSTANT)

σ_h (μ m)	l_c (μ m)	σ_s	H_D(μ m)	ε_{r1}	ε_{r2}
0.4	1.6293	0.0875	5	5	3
0.4	3.2586	0.1736	5	5	3
0.4	4.0732	0.2679	5	5	3

1 is lossy. For lossless medium 1, M_{33} ($\approx M_{44}$) [Fig. 5(b)] and (M_{34} ($\approx -M_{43}$) not shown), are more sensitive than $M_{11}, M_{12} = M_{21}$, and M_{22} to variations in the dissipation of medium 2.

In the previous illustrations $\varepsilon_{r1} < \varepsilon_{r2}$ (for lossless media). In the next set of data, the effect of total internal reflection at interface h_{12} is examined. The effects of varying rms slopes and correlation lengths (with $\varepsilon_{r1} > \varepsilon_{r2}$) are illustrated in Fig. 6. The input parameters corresponding to Fig. 6 for M_{11} are given in Table VI. For the lossless layered structures the Mueller matrix elements (as functions of backscatter angles) decrease less rapidly when $\varepsilon_{r1} > \varepsilon_{r2}$ than when $\varepsilon_{r1} < \varepsilon_{r2}$ since for near grazing incident angles total internal reflection occurs at the lower interface when $\varepsilon_{r1} > \varepsilon_{r2}$.

IV. CONCLUDING REMARKS

Using the full-wave approach to scattering from irregular multilayered structures, the Mueller matrix elements are evaluated as functions of the backscatter angle for different rough surface parameters Figs. 1–3, different thickness of the coating materials Fig. 4, and different (complex) permittivities Figs. 5 and 6.

The Mueller matrix elements are more sensitive to the changes in the rms slope than to changes in the rms height. The element M_{34} ($\approx -M_{43}$) [Fig. 4(b)] is most sensitive to variations in the thickness of the coating layer (medium 1). This result could be used to estimate the thickness of the coating material. The magnitudes of the Mueller matrix elements are considerably more sensitive to changes in dissipation in the coating material (medium 1) than to changes in dissipation of the substrate (medium 2) [Fig. 5(a) and (b)] Effects of the total internal reflection at the lower interface h_{12} are also considered (Fig. 6).

APPENDIX A
EVALUATION OF THE INCOHERENT (MODIFIED) MUELLER MATRIX ELEMENTS

The first term in (9) is defined as

$$\left\langle S_U^{PQ} S_U^{RS^*} \right\rangle_i = \left\langle S_U^{PQ} S_U^{RS^*} \right\rangle - \left\langle S_U^{PQ} \right\rangle \left\langle S_U^{RS^*} \right\rangle \tag{A.1}$$

where, in view of the small slope assumption (10), (A.1) reduces to

$$\begin{aligned}
&\left\langle S_U^{PQ} S_U^{RS^*} \right\rangle \\
&= \int_{-L}^{L}\int_{-l}^{l}\int_{-L}^{L}\int_{-l}^{l} \left\{ \iint D_U^{PQ} D_U^{RS^*} P_2(\vec{n}^f, \vec{n}^i \mid n)\, d\vec{n} \right. \\
&\quad \times \iint \left[e^{(i\vec{k}_0^f - \vec{k}_0^i)\vec{r}_{s1}} - e^{i(\vec{k}_0^f - \vec{k}_0^i)\vec{r}_{s10}} \right] \\
&\quad \times \left[e^{i(\vec{k}_0^f - \vec{k}_0^i)\vec{r}'_{s1}} - e^{i(\vec{k}_0^f - \vec{k}_0^i)\vec{r}'_{s10}} \right]^* \\
&\quad \left. \times\, p(h_{s1}, h'_{s1})\, dh_{s1}, dh'_{s1} \right\} dx_s\, dz_s\, dx'_s\, dz'_s \\
&= I_1 \int_{-L}^{L}\int_{-l}^{l}\int_{-L}^{L}\int_{-l}^{l} \left\{ \iint (e^{i\vec{k}_{d0}\cdot\vec{r}_{s1}} - e^{i\vec{k}_{d0}\cdot\vec{r}_{s10}}) \right. \\
&\quad \times (e^{i\vec{k}_{d0}\cdot\vec{r}'_{s1}} - e^{-i\vec{k}_{d0}\cdot\vec{r}'_{s10}}) \\
&\quad \left. \times\, p(h_{s1}, h'_{s1})\, dh_{s1},\, dh'_{s1} \right\} dx_s\, dz_s\, dx'_s\, dz'_s
\end{aligned} \tag{A.2}$$

where the large radii of curvature assumption has been made. The scattering coefficients are slowly varying functions of slope. Furthermore, $\vec{k}_{dj}$ is given by (12a) and

$$I_1 = \iint D_U^{PQ} D_U^{RS^*} P_2(\vec{n}^f, \vec{n}^i \mid \vec{n})\, d\vec{n}. \tag{A.3}$$

The radar footprint is $x_s \in [-l, l]$ and $z_s \in [-L, L]$. Thus [5],

$$\begin{aligned}
\left\langle S_U^{PQ} S_U^{RS^*} \right\rangle = I_1 \int_{-L}^{L}\int_{-l}^{l}\int_{-L}^{L}\int_{-l}^{l} &[\chi_2(v_{y0}, -v_{y0}; R) \\
&- \chi(u_{y0}) e^{iv_{y0}h_{01}} - \chi(-v_{y0}) e^{iv_{y0}h_{01}} + 1] \\
&\times e^{i(v_{x0}x_d + v_{z0}z_d)}\, dx_s\, dz_s\, dx'_s\, dz'_s.
\end{aligned} \tag{A.4}$$

where $\chi_z(a, b; R)$ is the joint characteristic function and $\chi(a)$ is the characteristic function. The coherent contribution can be expressed as

$$\begin{aligned}
\left\langle S_U^{PQ} \right\rangle \left\langle S_U^{PQ} \right\rangle^* &= \left\langle \lim_{|r_d| \to \infty} S_U^{PQ} S_U^{RS^*} \right\rangle \\
&= \left\langle \lim_{|R| \to 0} S_U^{PQ} S_U^{RS^*} \right\rangle
\end{aligned} \tag{A.5}$$

where $r_d = (x_d^2 + z_d^2)^{1/2}$ and $R(r_d)$ is the normalized rough surface height autocorrelation function (isotropic surface). Furthermore,

$$\begin{aligned}
\lim_{|r_d| \to \infty} \chi_2(a, b; R) &= \lim \chi_2(a, b; R)_{|R| \to 0} \\
&= \chi_2(a, b, 0) = \chi(a)\chi(b).
\end{aligned} \tag{A.6}$$

Thus

$$\langle S_U^{PQ}\rangle\langle S_U^{PQ}\rangle^* = I_1 \int_{-L}^{L}\int_{-l}^{l}\int_{-L}^{L}\int_{-l}^{l}[\chi(v_{y0})\chi(-v_{y0}) - \chi(v_{y0}) \times e^{-iv_{y0}h_{01}} - \chi(-v_{y0})e^{iv_{y0}h_{01}} + 1] \times e^{i(v_{x0}x_d + v_{z0}z_d)}\,dx_s\,dz_s\,dx_s'\,dz_s'. \quad \text{(A.7)}$$

Therefore, the incoherent scattered power is

$$\langle S_U^{PQ} S_U^{PQ^*}\rangle_i = I_1 \int_{-L}^{L}\int_{-l}^{l}\int_{-L}^{L}\int_{-l}^{l}[\chi_2(v_{y0} - v_{y0}) - \chi(v_{y0})\chi(-v_{y0})] \times e^{i(v_{x0}x_d + v_{z0}z_d)}\,dx_s\,dz_s\,dx_s'\,dz_s'. \quad \text{(A8)}$$

The four-dimensional integrals (A.8) are reduced to 2-D integrals upon changing the integration variables (assuming that the random rough surface characteristics are homogeneous)

$$x_d = x_s - x_s' \quad x_a = (x_s - x_s')/2 \quad z_d = z_s - z_s' \quad z_a = (z_s - z_s')/2 \quad \text{(A.9)}$$

$$\langle S_U^{PQ} S_U^{RS^*}\rangle_i = I_1 \int_{-2L}^{2L}\int_{-2l}^{2l}(2l - |x_d|)(2L - |z_d|)[\chi_2(v_{y0} - v_{y0}) - \chi(v_{y0})\chi(-v_{y0})]e^{i(v_{x0}x_d + v_{z0}z_d)}\,dx_d\,dz_d \quad \text{(A.10)}$$

where I_1 is as follows:

$$I_1 = \iint \left| D_{00U}^{PQ} + D_{01U}^{PQ}e^{-2v_1^i H_D} + D_{10U}^{PQ}e^{-i2v_1^f H_D} + D_{11U}^{PQ}e^{-i2(v_1^i + v_1^f)H_D}\right|^2 P_2(\vec{n}^f, \vec{n}^i \mid n)\,d\vec{n}. \quad \text{(A.11)}$$

The individual terms of I (11b) are defined in (12b). The other three terms in (9) are expressed in a similar manner.

ACKNOWLEDGMENT

The authors would like to thank R. Vietz and J. Craig for their work in preparing this manuscript.

REFERENCES

[1] G. G. Stokes, "On the composition and resolution of streams of polarized light from different sources," *Trans. Cambridge Phil. Soc.*, vol. 9, pp. 399–416, 1852 (reprinted in *Mathematical and Physical Papers*. London, U.K.: Cambridge Univ. Press, 1901, vol. 3, pp. 233–250.

[2] E. Collet, *Polarized Light: Fundamentals and Applications*. New York: Marcel Dekker, 1992.

[3] E. Bahar and Y. Zhang, "Like and cross polarized fields diffusely scattered from irregular layered structures," *Trans. Antennas Propagat.*, this issue, pp. 941-948.

[4] A. Ishimaru, *Wave Propagation and Scattering in Random Media*. New York: Academic, 1978.

[5] E. Bahar and B. S. Lee, "Full wave solutions for rough surface radar cross sections: Comparision with small perturbation, physical optics, numerical and experimental results," *Radio Sci.*, vol. 29, no. 2, pp. 407–429, Mar./Apr. 1994.

[6] D. E. Barrick and W. H. Peake, "A review of scattering from surfaces with different roughness scales," *Radio Sci.*, vol. 3, no. 8, pp. 865–868, 1968.

[7] M. I. Sancer, "Shadow-corrected electromagnetic scattering from a randomly rough surface," *IEEE Trans. Antennas Propagat.*, vol. AP-17, pp. 577–585, Sept. 1968.

[8] B. G. Smith, "Geometrical shadowing of a randomly rough surface," *IEEE Trans. Antennas Propagat.*, vol. AP-15, pp. 668–671, Sept. 1976.

Yuzhi Zhang, for a photograph and biography, see this issue, p. 948.

Ezekiel Bahar (S'63–M'64–SM'72–F'85), for a photograph and biography, see this issue, p. 948.